Available online at www.sciencedirect.com
ScienceDirect
Journal of Magnetic Resonance 187 (2007) 193–198
JMR Journal of Magnetic Resonance
www.elsevier.com/locate/jmr

Biselective refocusing pulses and the SERF experiment

Jean-Marc Nuzillard *

Institut de Chimie Moléculaire de Reims, BP 1039, 51687 REIMS Cedex 2, France

Received 19 March 2007; revised 25 April 2007
Available online 6 May 2007

Abstract

The SERF experiment is a variant of the homonuclear *J*-resolved experiment, in which a single coupling constant is measured. It consists of a single chemical shift selective excitation that is followed by a biselective spin echo. Recent articles mention the existence of artefacts in SERF spectra that are supposedly related to pulse imperfections. This article presents a detailed study of the biselective refocusing pulses. It also reports a method for predicting the position and amplitude of the expected and unexpected 2D spectral peaks in SERF spectra. Artefacts can be partially eliminated by phase cycling or by the introduction of static field gradient pulses in the acquisition sequence. A procedure to obtain of pure absorption peaks in SERF spectra is proposed.

Keywords: Liquid state NMR; Selective pulses; *J*-Spectroscopy; Spin echo; Linear prediction

1. Introduction

The measurement of coupling constants in liquid state NMR is a topic that has recently regained interest, due to the emergence of new experimental methods for residual dipolar coupling observation [1,2]. *J*-Resolved spectroscopy [3] offers an elegant way to untangle complex coupling patterns, and therefore to facilitate the study of complex molecules. The SERF (SElective ReFocusing) experiment [4] was designed to focus on a single coupling at a time. Strong coupling artefacts in homonuclear *J*-spectroscopy have been thoroughly discussed in the literature and an efficient way to suppress them has recently been proposed [5]. The SERF experiment however produces artefacts, even when it is applied to weakly coupled systems. This observation is generally interpreted in terms of "pulse imperfections". The goal of this article is to provide a detailed description of what these imperfections are, and to propose a very simple way of partially eliminating them. Understanding the spin dynamics that take place during selective refocusing has allowed the development of a method to obtain pure absorption peaks in SERF spectra.

2. Theory

The pulse sequence of the SERF experiment is reported in Fig. 1. The studied two-spin system is weakly coupled, offsets of nuclei I and S are $+\omega_0$ and $-\omega_0$, and their coupling constant is J. The effect of the spin echo on the initial $-I_y$ spin state is considered in the subset of the single transition operator base [6] that only contains ± 1 quantum states:

$$\mathcal{B}^{(\pm 1)} = \{I_- S_\alpha, I_\alpha S_-, I_- S_\beta, I_\beta S_-, I_+ S_\alpha, I_\alpha S_+, I_+ S_\beta, I_\beta S_+\} \quad (1)$$

Each operator in this base is an eigenoperator of the superoperators that are associated with chemical shift and coupling interactions. Choosing $\mathcal{B}^{(\pm 1)}$ as base thus concentrates the theoretical analysis on the study of the biselective refocusing pulse behavior.

A single site selective shaped pulse of duration τ, defined by its $\omega_1^m(t) = \gamma B_1^m(t)$ intensity profile, is transformed into a two site selective shaped pulse by cosine modulation at angular frequency ω_0 [7], in order to similarly and simultaneously act at offsets $+\omega_0$ and $-\omega_0$:

* Fax: +33 0 3 26 91 25 96.
E-mail address: jm.nuzillard@univ-reims.fr

1090-7807/$ - see front matter © 2007 Elsevier Inc. All rights reserved.
doi:10.1016/j.jmr.2007.05.001

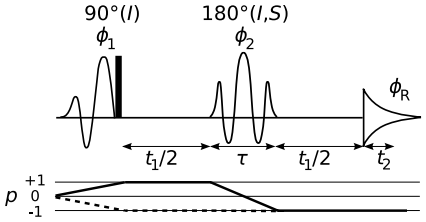

Fig. 1. The original SERF pulse sequence. The black rectangle is a purging pulse that may be omitted, according to the authors of Ref. [2]. The soft excitation pulse (the first one) is singly selective and the soft refocusing pulse (the second one) is doubly selective. The original phase cycling is $\phi_1 = x, -x$, $\phi_2 = x$ and $\phi_R = x, -x$ with phase alternation of the purging pulse ($\phi = \pm y$ without changing ϕ_R). This leads to the preservation of both transfer coherence pathways, in solid and dashed lines. The basic phase cycling of the SERFS is $\phi_1 = x$, $\phi_2 = x, y, -x, -y$ and $\phi_R = x, -x$; it solely preserves the coherence transfer pathway in solid line.

$$\gamma B_1(t) = \omega_1(t) = 2\omega_1^m(t)\cos\left(\omega_0\left(t - \frac{\tau}{2}\right)\right) = 2\omega_1^m(t)\cos(\omega_0 t') \tag{2}$$

The modulation of a refocusing pulse is achieved so that its overall phase is defined in the middle, when $t' = 0$. Considering that $|\omega_1^m(t)| \ll 2\omega_0$, or equivalently that what I experiences does not interfere with what S experiences, the time-dependent Hamiltonian that describes the evolution of the spin system during the refocusing period can be written as:

$$\begin{aligned}\mathcal{H}_1(t) = {} & \pi J 2 I_z S_z + \omega_0(I_z - S_z) \\ & + \omega_1^m(t)[(\cos(\omega_0 t')I_x + \sin(\omega_0 t')I_y)] \\ & + \omega_1^m(t)[(\cos(\omega_0 t')S_x - \sin(\omega_0 t')S_y)]\end{aligned} \tag{3}$$

The similarity transformation that is defined by

$$U(t) = \exp(\mathrm{i}\omega_0(I_z - S_z)t') \tag{4}$$

solves the problem of spin state evolution under $\mathcal{H}_1(t)$ between times $t_1/2$ and $t_1/2 + \tau$:

$$\sigma(t_1/2 + \tau) = U^{-1}(\tau)P(\tau)U(0)\sigma(t_1/2)U^{-1}(0)P(\tau)^{-1}U(\tau) \tag{5}$$

in which $P(\tau)$ is the propagator of the interaction representation Hamiltonian $\mathcal{H}^r$:

$$\mathcal{H}^r = \pi J 2 I_z S_z + \omega_1^m(t)(I_x + S_x). \tag{6}$$

The RF field is symmetrically modulated around the middle of the pulse and therefore

$$U^{-1}(\tau) = U(0) = \exp(-\mathrm{i}\omega_0(I_z - S_z)\tau/2) \tag{7}$$

meaning that what happens during the pulse can be analyzed as a three step process:

1. Action of only the chemical shift operator $\omega_0(I_z - S_z)$ during time $\tau/2$
2. Action of $\mathcal{H}^r$ during time τ
3. Action of only the chemical shift operator during time $\tau/2$, again.

When the whole spin echo is now considered, the free evolution period and similarity transformation actions can be grouped together in the $P(t_1 + \tau)$ propagator:

$$\begin{aligned}&\sigma(t_1 + \tau) = P(t_1 + \tau)\sigma(0)P^{-1}(t_1 + \tau) \\ &P(t_1 + \tau) = P_\omega P_J P(\tau) P_J P_\omega \\ &P_\omega = \exp(-\mathrm{i}\omega_0(t_1 + \tau)(I_z - S_z)/2) \\ &P_J = \exp(-\mathrm{i}\pi J t_1 2 I_z S_z/2)\end{aligned} \tag{8}$$

The representation of the P_ω propagator action on $\mathcal{B}^{(\pm 1)}$ base elements is given by a diagonal matrix, because these elements are coherences of the spin system. The same remark holds for P_J. There is no straightforward analytical solution for the representation of $P(\tau)$ when $\mathcal{H}^r$ depends on time through the envelope shape function $\omega_1^m(t)$.

The matrix representation of the action of the propagator $P(\tau)$ in the bases

$$\begin{aligned}&\mathcal{B}^{(2)} = \{I_x - S_x, 2I_yS_z - 2I_zS_y\} \\ &\mathcal{B}^{(3)} = \{I_x + S_x, 2I_yS_z + 2I_zS_y, 2I_zS_z - 2I_yS_y\} \\ &\mathcal{B}^{(4S)} = \{I_y + S_y, 2I_xS_z + 2I_zS_x, I_z + S_z, 2I_xS_y + 2I_yS_x\} \\ &\mathcal{B}^{(4A)} = \{I_y - S_y, 2I_xS_z - 2I_zS_x, I_z - S_z, 2I_xS_y - 2I_yS_x\}\end{aligned} \tag{9}$$

was derived from reference [8]. The corresponding matrices are noted $R^{(2)}$, $R^{(3)}$, $R^{(4S)} = R^{(4A)} = R^{(4)}$. For completeness, it must be noted that operators $2I_xS_x$ and $2I_yS_y + 2I_zS_z$ are left unchanged by $\mathcal{H}^r$.

Each operator in $\mathcal{B}^{(\pm 1)}$ is transformed by $\mathcal{H}^r$ into a linear combination of single transition operators that are not all related to ± 1 quantum transitions. Indeed, $R^{(\pm 1)}$, the matrix representation of $P(\tau)$ in $\mathcal{B}^{(\pm 1)}$, reflects the action of $P(\tau)$ when followed by the projection in the subspace that is spanned by $\mathcal{B}^{(\pm 1)}$. Writing $R^{(\pm 1)}$ requires the definition of C, a real number and of z_0, z_e and z_1, three complex numbers, from the seven matrix elements $R_{11}^{(2)}$, $R_{21}^{(2)}$, $R_{11}^{(3)}$, $R_{21}^{(3)}$, $R_{22}^{(3)}$, $R_{11}^{(4)}$ and $R_{22}^{(4)}$:

$$\begin{aligned}8C &= R_{11}^{(3)} - R_{22}^{(3)} \\ 8z_0 &= \left(2R_{11}^{(2)} + R_{11}^{(3)} + R_{22}^{(3)} - 4R_{11}^{(4)}\right) + 2\mathrm{i}\left(R_{21}^{(2)} + R_{21}^{(3)} + 2R_{21}^{(4)}\right) \\ 8z_e &= \left(-2R_{11}^{(2)} + R_{11}^{(3)} + R_{22}^{(3)}\right) - 2\mathrm{i}\left(R_{21}^{(2)} - R_{21}^{(3)}\right) \\ 8z_1 &= \left(2R_{11}^{(2)} + R_{11}^{(3)} + R_{22}^{(3)} + 4R_{11}^{(4)}\right) + 2\mathrm{i}\left(R_{21}^{(2)} + R_{21}^{(3)} - 2R_{21}^{(4)}\right)\end{aligned} \tag{10}$$

The matrix $R^{(\pm 1)}$ is obtained after a simple but lengthy calculation and its elements are given by Table 1. This result takes into account the time symmetrical nature of the pulse shape function $\omega_1^m(t)$, thus allowing to write the matrix element equality: $R_{12}^{(3)} = -R_{21}^{(3)}$.

After a first pulse of phase x, the spin state at the beginning of the echo is $\sigma_0 = -I_y$:

$$-2\mathrm{i}\sigma_0 = I_+S_\alpha + I_+S_\beta - I_-S_\alpha - I_-S_\beta. \tag{11}$$

Each of the four operators in σ_0 is transformed during time $t_1 + \tau$ into a combination of the four -1 quantum single transition operators of the spin system and into other terms

Table 1
Matrix representation of the action of the Hamiltonian operator $\mathcal{H}'$ during pulse time τ, expressed in the base of ± 1 single transition operators

$\mathcal{H}'$ ↙	I_-S_α	$I_\alpha S_-$	I_-S_β	$I_\beta S_-$	I_+S_α	$I_\alpha S_+$	I_+S_β	$I_\beta S_+$
I_-S_α	z_1	z_e	C	C	C	C	z_0	z_e
$I_\alpha S_-$	z_e	z_1	C	C	C	C	z_e	z_0
I_-S_β	C	C	$\bar{z}_1$	$\bar{z}_e$	$\bar{z}_0$	$\bar{z}_e$	C	C
$I_\beta S_-$	C	C	$\bar{z}_e$	$\bar{z}_1$	$\bar{z}_e$	$\bar{z}_0$	C	C
I_+S_α	C	C	$\bar{z}_0$	$\bar{z}_e$	$\bar{z}_1$	$\bar{z}_e$	C	C
$I_\alpha S_+$	C	C	$\bar{z}_e$	$\bar{z}_0$	$\bar{z}_e$	$\bar{z}_1$	C	C
I_+S_β	z_0	z_e	C	C	C	C	z_1	z_e
$I_\beta S_+$	z_e	z_0	C	C	C	C	z_e	z_1

See text for the explanation about the values of C, z_0, z_e and z_1.

that cannot lead to observable signals. Therefore, the SERF spectrum of this spin system presents 16 peaks. For example, by application of Eq. (8), the intensity of the transfer from I_+S_α to I_-S_β is obtained as follows:

$$\begin{aligned} P_\omega(I_+S_\alpha)P_\omega^{-1} &= \exp(-\mathrm{i}\omega_0(t_1+\tau)/2)(I_+S_\alpha) \\ P_J(I_+S_\alpha)P_J^{-1} &= \exp(-\mathrm{i}\pi J t_1/2)(I_+S_\alpha) \\ P(\tau)(I_+S_\alpha)P(\tau)^{-1} &= \bar{z}_0(I_-S_\beta)+\ldots \\ P_J(I_-S_\beta)P_J^{-1} &= \exp(-\mathrm{i}\pi J t_1/2)(I_-S_\beta) \\ P_\omega(I_-S_\beta)P_\omega^{-1} &= \exp(+\mathrm{i}\omega_0(t_1+\tau)/2)(I_-S_\beta) \end{aligned} \quad (12)$$

leading to a transformation of I_+S_α to $\bar{z}_0\exp(-\mathrm{i}\pi J t_1)I_-S_\beta$. The latter term evolves during acquisition at the angular frequency $\omega_0-\pi J$. The SERF spectrum thus contains a peak of intensity $\bar{z}_0$ at frequencies $(\Omega_1,\Omega_2)=(-\pi J, \omega_0-\pi J)$. Similar calculations lead to the schematic 2D spectrum in Fig. 2a. Peak intensities in the magnitude mode spectrum are $|C|$, F_0, F_e and F_1.

$$F_0=|z_0|, \quad F_e=|z_e|, \quad F_1=|z_1| \quad (13)$$

It clearly appears that if the coherence transfers that are caused by the soft refocusing pulse are restricted to the $+1$ to -1 pathway (see Fig. 1), then the number of 2D peaks reduces from sixteen to eight. The useful part of the initial spin state σ_0 then only contains two single transition operators: I_+S_α and I_+S_β, instead of four. Such a restriction is achieved either by phase cycling or by inserting two identical field gradient pulses around the soft refocusing pulse. The corresponding experiment is named SERFS (for SERF with coherence transfer Selection). Its phase program is given in the caption of Fig. 1. It produces the spectrum that is sketched in Fig. 2b. After tilt and symmetrization, only four peaks remain, the two expected ones and two other ones that are located on the $\Omega_1=0$ axis (see Fig. 2c).

When only considering the action of the biselective pulse during time τ on operators I_+S_α and I_+S_β to produce operators I_-S_β and I_-S_α, everything happens as if the spin system was subjected to an ideal spin echo sequence of duration $\lambda\tau$ (see Fig. 3). Idealness is defined here by the conditions $F_0\approx 1$ and $C\approx 0$, that are fulfilled in practical situations (see below). Of course, this model does not

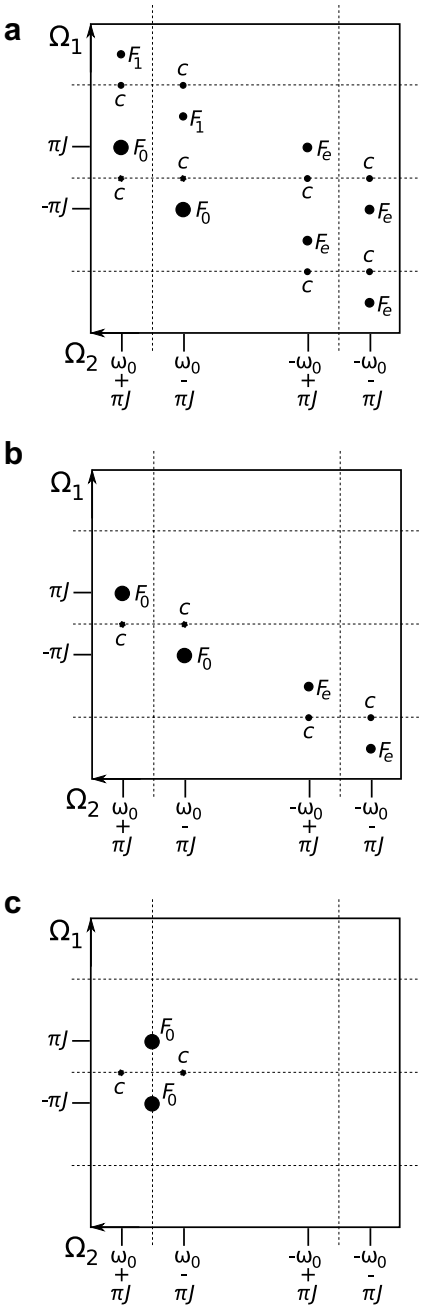

Fig. 2. (a) Schematic representation of the SERF spectrum of a weakly coupled two spin system, (b) the corresponding SERFS spectrum, (c) SERFS spectrum after tilt and symmetrization.

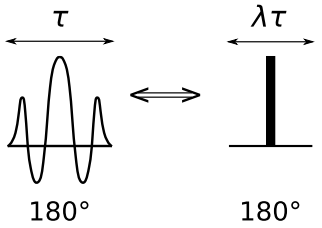

Fig. 3. Theoretical equivalence between a soft biselective refocusing pulse of duration τ and an ideal spin echo of duration $\lambda\tau$. See text for the limits of such an equivalence.

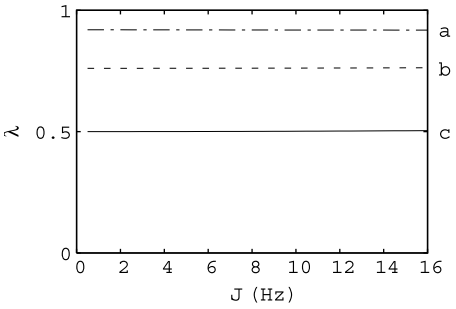

Fig. 4. Graphs of the pulse λ parameter as a function of the active coupling constant J, for the three pulses in Table 2. (a) RE-BURP, (b) Gaussian, (c) rectangular.

account for the magnetization transfer from I to S (and *vice versa*), whose intensity depends on z_e.

The dimensionless parameter λ is given by:

$$\lambda\pi J\tau = \arg(z_0) \bmod 2\pi \tag{14}$$

In practice, the value of λ does not depend on J, thus proving the pertinence of the soft pulse model in Fig. 3, as shown in Fig. 4.

A SERFS experiment in which the t_1 increment dt_1 is chosen so that

$$dt_1 = n\lambda\tau \quad n \in \mathbb{N} \tag{15}$$

is equivalent, for the I nucleus only, to an unselective J-resolved spectrum in which the first n FIDs are missing. After Fourier transformation of the SERFS raw data in the Ω_2 dimension, the missing first n spectra can artificially be obtained by backward linear prediction [9]. A second step of linear prediction, toward negative t_1 values, leads to a pure absorption SERF spectrum, according to the principle of the ALPESTRE method (www.univ-reims.fr/LSD/JmnSoft/Alpestre) [10].

3. Experimental

SERF and SERFS spectra were recorded on a Bruker DRX spectrometer operating at 500.13 MHz for the ^{1}H nucleus. The sample was made of 10 mg of cinnamic acid dissolved in 0.7 mL of deuterated chloroform. The two ethylenic protons at 7.86 and 6.53 ppm shared a single scalar coupling of intensity $J = 15.96$ Hz. Their resonance frequency difference $2\omega_0/2\pi = 669.2$ Hz was high enough relative to J to consider that these nuclei form a weakly coupled spin system. The initially selected signal was that at 7.86 ppm.

The basic pulse sequences in Fig. 1 was modified by replacing the initial soft pulse by a hard one of phase ϕ_1, followed by a single site selective DPFGSE sequence [11]. The latter contained two 1% truncated Gaussian pulses (50 ms each) [12] and two pairs of gradient pulses (1 ms, 38 and 10 G cm^{-1} for the first and the second pair, respectively). This method was chosen because it presented a much better selectivity than the original one, in which the initial excitation was achieved by an E-BURP pulse [13].

The duration of the RE-BURP [13] refocusing pulse was 100 ms. Its envelope was amplitude modulated at 334.6 Hz to achieve the desired double refocusing profile.

In order to visualize artifacts at their true position (without folding in the indirect dimension), all spectral widths were set to 1 kHz for the spectra in Fig. 5. The acquisition matrices contained 512×2K points. Each FID was recorded by co-adding 8 transients separated by 2.5 s relaxation delays. A sine bell pseudo echo filter was applied in both dimensions prior to Fourier transformation and magnitude calculation. Final spectral matrice size was $1\text{K} \times 1\text{K}$ points.

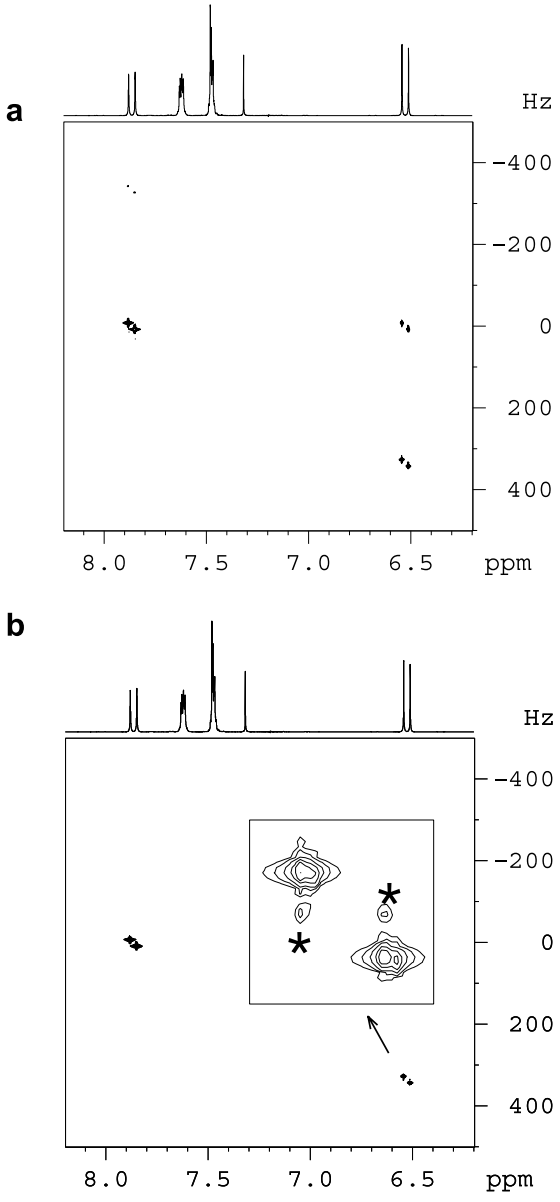

Fig. 5. The SERF (a) and SERFS (b) spectra of the ethylenic protons of cinnamic acid. The chemical shift of the initially excited one is 7.86 ppm. The zoomed area in spectrum (b) was drawn to show the peaks of low intensity C, marked by $*$ symbols. They also appears in spectrum (a).

The SERFS spectra in Fig. 6 were recorded in identical conditions as Fig. 5b, but with a spectral width of 54.44 Hz in dimension 1. The dt_1 increment of t_1 is therefore 18.4 ms. Considering that the λ value of the 100 ms RE-BURP pulse is 0.92, the value of n in Eq. (15) is 5. After Fourier transformation in dimension 2 (size: 1K complex points), the first 360 columns of the data set were extracted to only process the signals of the initially excited nuclei. The five missing spectra were calculated using modified routines of the ALPESTRE software package (www.univ-reims.fr/LSD/JmnSoft/Alpestre). After phasing the 2D data set along dimension 2, the unmodified ALPESTRE algorithm was applied.

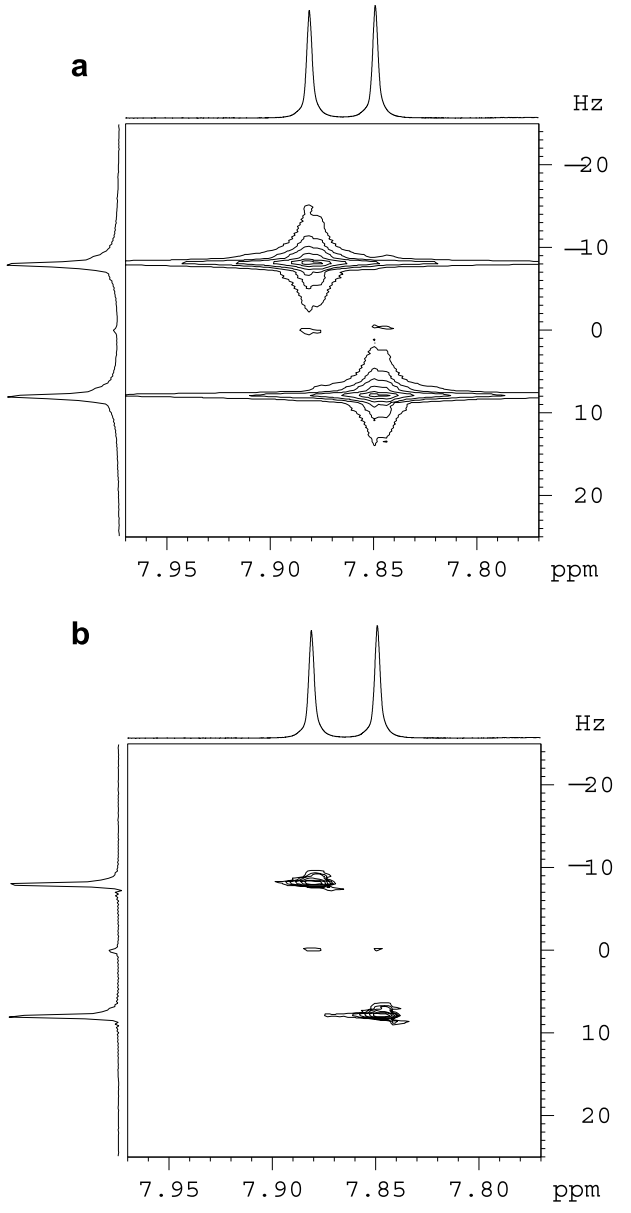

Fig. 6. The SERFS data set of the ethylenic proton at 7.86 ppm was processed (a) in the magnitude mode and without application of any apodization filter, (b) using backward linear prediction to reconstruct the five missing initial t_1 increments (see text) and then ALPESTRE to produce double absorption peaks.

4. Results and discussion

The main theoretical result of this article is summarized in Table 1. The transformation of the base $\mathcal{B}^{(\pm 1)}$ of ± 1 quantum states by $\mathcal{H}^r$ followed by the projection in the same base is fully determined by the three complex numbers z_0, z_e and z_1, and by the real number C. The factor z_0 or its complex conjugate intervene for the expected transformation, that is the simultaneous exchange of the $+$ and $-$ state labels for one nucleus, and of the α and β state labels for the other one (e.g. I_-S_α to I_+S_β). The factor z_e characterizes the magnetization transfer between nuclei, either without spin state label change (I_-S_α to $I_\alpha S_-$) or with both spin state label changes (I_-S_α to $I_\beta S_+$). The e index in z_e was given in reference to a degree of ellipticity in the biselective pulse behavior, and more precisely because the combinations $I_x + S_x$ and $I_x - S_x$ are transformed by $\mathcal{H}^r$ according to different variation laws. This behavior difference is obviously the origin of the observed magnetization transfer between nuclei. The preservation of the spin state (I_-S_α to I_-S_α) is ruled by the value of z_1. The pathway that preserves the coherence order is eliminated in the SERFS experiment, in contrast to the SERF experiment in which all transfers are allowed. All other transfer intensities are governed by C, whose value is not of great practical importance, as shown hereafter.

The values of the four pulse parameters depend on the $J\tau$ product, and on the pulse shape function. They can be calculated using a computer program that is free at www.univ-reims.fr/LSD/JmnSoft/Bisel. The three complex numbers are displayed as their modulus (F values) and argument (θ values). A shape function $\omega_1^m(t)$ is calculated from the corresponding shape file (in Bruker format), whose values are rescaled to build a refocusing pulse, so that

$$\frac{\tau}{N}\sum_{k=1}^{N}\omega_1^m(\tau_k) = \pi \tag{16}$$

The program checks that all pulse parts have either a zero or a π phase and that the shape is symmetrical around $\tau/2$.

Three shapes are theoretically considered for comparison purpose: rectangular, Gaussian [12] and RE-BURP [13]. The chosen experimental conditions involve a coupling constant of 10 Hz and a selection band width of 50 Hz. The latter is defined between the null crossing points of the inversion profile, when calculated for an isolated spin. The magnitudes of the magnetization transfers are given in Table 2. For the chosen selection band width, the obtained values are equivalent. The C values are small enough to be considered as practically null. Conversely, F_e cannot be neglected, comparatively to F_0. The corresponding artefact pairs in SERF spectra that lie around the $\omega_1 = 0$ axis are not present in the SERFS spectra. The

Table 2
True peak and artefact intensity in SERF and SERFS spectra for which $J = 10$ Hz and refocusing pulses have a 50 Hz inversion band width

Shape	τ (ms)	F_0	F_e	F_1	C	λ
Rectangular	16	0.984	0.124	0.016	2.5×10^{-5}	0.50
Gaussian	30	0.987	0.111	0.013	8.5×10^{-5}	0.76
RE-BURP	109	0.978	0.137	0.019	1.4×10^{-3}	0.92

The table also gives the pulse length τ that achieves the desired selectivity and the pulse λ value.

other artefact pairs of intensity F_e have no symmetrical counterpart and can be easily identified or eliminated by tilt and symmetrization.

The theoretical predictions are fully supported by experiments. The SERF and SERFS spectra in Figs. 5a and b match the schematic representations in Figs. 2a and b.

Knowing the λ parameter of the used refocusing pulse allows to adequately choose an acquisition spectral width along the Ω_1 axis that is compatible with the production of pure absorption 2D SERFS peaks. Fig. 6a shows how the raw data set is transformed by the standard magnitude mode method, with no apodization filter applied. The spectrum in Fig. 6b clearly demonstrates that the same data set is more efficiently transformed when the linear prediction and ALPESTRE algorithms are used.

Finally, the value of λ characterizes how a pulse "fills" its lifetime. The rectangular pulse, especially when $\omega_1^m \gg \pi J$, fills it to its maximum. Under these circumstances, it can easily been shown that everything happens as if the coupling constant acted during half of the time, or equivalently, as if the effective J value were $J/2$. The value of λ is then close to 1/2. In shaped (non-rectangular) pulses, there are periods of time in which the coupling interaction is more efficient, when $\omega_1^m(t) \leqslant \pi J$, because the coupling interaction is less masked by the action of the RF field. When the fully-efficient-J versus the half-efficient-J time ratio is high (as in RE-BURP), the value of λ can be close to 1. The 1% truncated Gaussian pulse ($\lambda = 0.76$) represents an intermediate case between a rectangular pulse and a RE-BURP pulse.

5. Conclusion

The analysis of artefacts in the SERF spectrum leads to the proposal of a detailed description of biselective refocusing pulses. The intensity of the coherence transfers they cause can be predicted from the value of the coupling constant, from the pulse length and from the shape of the pulse envelope. Artefacts in SERF spectra are partially removed by phase cycling or by the introduction of gradient pulses in the sequence, in order to preserve the only coherence transfer pathway of interest. Pure absorption lineshape SERFS spectra can be obtained by a careful selection of acquisition and processing protocols, through shaped pulse parameter calculations and linear prediction based signal processing.

Acknowledgment

I thank Dr. K. Plé for linguistic advice.

References

[1] J. Farjon, D. Merlet, P. Lesot, J. Courtieu, Enantiomeric excess measurements in weakly oriented chiral liquid crystal solvents through 2D ^{1}H selective refocusing experiments, J. Magn. Reson. 158 (2002) 169–172.
[2] L. Beguin, J. Courtieu, L. Ziani, D. Merlet, Simplification of the ^{1}H NMR spectra of enantiomers dissolved in chiral liquid crystals, combining variable angle sample spinning and selective refocusing experiments, Magn. Reson. Chem. 44 (2006) 1096–1101.
[3] W.P. Aue, J. Karhan, R.R. Ernst, Homonuclear broad band decoupling and two-dimensional J-resolved NMR spectroscopy, J. Chem. Phys. 64 (1976) 4226–4227.
[4] T. Fäcke, S. Berger, SERF, a new method for H,H spin-coupling measurement in organic chemistry, J. Magn. Reson. A 113 (1995) 114–116.
[5] M.L. Thrippleton, R.A.E. Edden, J. Keeler, Suppression of strong coupling artefacts in J-spectra, J. Magn. Reson. 174 (2005) 97–109.
[6] R.R. Ernst, G. Bodenhausen, A. Wokaun, Principles of Nuclear Magnetic Resonance in One and Two Dimensions, Clarendon Press, Oxford, 1987.
[7] L. Emsley, I. Burghardt, G. Bodenhausen, Double selective inversion in NMR and multiple quantum effects in coupled spin systems, J. Magn. Reson. 90 (1990) 214–220.
[8] V. Blechta, J. Schraml, Response of a coupled two-spin system to on-resonance amplitude modulated RF pulses, Mol. Phys. 87 (1996) 679–689.
[9] J.J. Led, H. Gesmar, Application of the linear prediction method to NMR spectroscopy, Chem. Rev. 91 (1991) 1413–1426.
[10] J.-M. Nuzillard, Time-reversal of NMR signals by linear prediction. Application to phase-sensitive homonuclear J-resolved spectroscopy, J. Magn. Reson. A 118 (1996) 132–135.
[11] T.-L. Hwang, A.J. Shaka, Water suppression that works. Excitation sculpting using arbitrary waveforms and pulsed field gradients, J. Magn. Reson. A (1995) 275–279.
[12] C.J. Bauer, R. Freeman, T. Frenkiel, J. Keeler, A.J. Shaka, Gaussian pulses, J. Magn. Reson 58 (1984) 442–457.
[13] H. Geen, R. Freeman, Band-selective radiofrequency pulses, J. Magn. Reson. 93 (1991) 93–141.